Annu. Rev. Phys. Chem. 1991. 42: 369–92

MULTIDIMENSIONAL INTERMOLECULAR POTENTIAL SURFACES FROM VIBRATION-ROTATION-TUNNELING (VRT) SPECTRA OF VAN DER WAALS COMPLEXES

Ronald C. Cohen and Richard J. Saykally

Department of Chemistry, University of California, Berkeley, California 94720

KEY WORDS: intermolecular potentials, van der Waals complexes

INTRODUCTION

The role of intermolecular forces in modern science is becoming ever more prominent, as increasing numbers of chemists and physicists turn to the investigation of condensed matter phenomena and biological systems. Although the subject is hardly novel, the state of our knowledge of intermolecular forces and their associated potential energy surfaces is, nevertheless, remarkably primitive. For example, isotropic descriptions of the pairwise interactions between most of the common small molecules have existed for many years, but the anisotropy of these interactions still remains largely uncharacterized—even after nearly two decades of investigation with the most sophisticated experimental and theoretical techniques available! Furthermore, anisotropy is a dominant feature of systems that have the most significance, viz. those exhibiting hydrogen bonding.

This state of affairs seems all the more surprising when one considers that detailed theoretical formulations have been developed (1) for describing the three types of weak attractive interactions that occur between a pair of molecules, viz. electrostatic, induction, and dispersion forces, and that at least the low-order parameters that describe these interactions (polarizabilities, dipole moments, quadrupole moments) are generally well-known. However, as we elaborate upon in this review, it is our lack of

0066–426X/91/1101–0369$02.00

knowledge of the higher-order terms in the radial and multipole expansions of the attractive forces and of the anisotropic components of the exchange repulsion that preclude a more complete understanding of intermolecular forces.

The use of modern high-resolution spectroscopy and molecular beam techniques for the study of intermolecular forces has been reviewed recently by Hutson (2). Microwave spectroscopy has now been employed in the study of a large collection of weakly bound complexes (3). Although this collective work has given us considerable qualitative insight into the nature of weak intermolecular anisotropy, microwave spectra do not explore sufficiently large ranges of the large amplitude coordinates to permit the extraction of an accurate intermolecular potential energy surface (IPS). Mid- and near-infrared (IR) laser methods have similarly been used to study many weakly bound complexes over the last decade. The difficulty with this approach is that it usually does not probe the large amplitude coordinate of the complexes with sufficient sensitivity, and only in very special cases has a ground state IPS actually been extracted from such experiments. Dramatic progress in this area has been realized in the last few years (4, 5), however, wherein the capability has been developed to study low frequency vibrations in complexes through hotbands and combination bands associated with the monomer fundamentals (6). As Hutson (2) discussed, the use of molecular beam scattering methods and other techniques for studying intermolecular forces suffer from a variety of other limitations.

During the last several years, the rapid development for far-IR laser spectroscopic techniques, which are capable of measuring the low-frequency vibrations of the van der Waals bonds in weakly bound complexes (7–10), has produced an extensive new data base, from which the intimate details of intermolecular interactions can be deduced, at least in principle. We call this new approach vibration-rotation-tunneling (VRT) spectroscopy, because the transitions that are measured are either stretching vibrations of the van der Waals bonds, or hindered rotation-tunneling states of the constituent monomers; hence, the terminology is generally applicable to all weakly bound complexes.

The design and construction of tunable far-IR laser of spectrometers used for VRT spectroscopy has been described in detail in a recent review (11, 12). The investigations of weakly bound complexes, conducted by the four groups currently pursuing far-IR-VRT spectroscopy, is detailed in a separate review (13). In Table 1, we list the molecules studied to date by this method and the appropriate references.

To actually extract a detailed characterization of intermolecular forces from VRT spectra, a general mathematical inversion scheme must exist

Table 1 Clusters that have been studied by tunable far-IR laser spectroscopy

Cluster	Reference	Cluster	Reference
ArHCl	7, 8, 9, 10	$(NH_3)_2$	27
ArHBr	14	H_2O-CO	28
ArH_2O	15–19	H_2O-N_2	29
$ArNH_3$	20–22	H_2O-CH_4	30
$(HCl)_2$	23, 24	Ar_2HCl	31
$(H_2O)_2$	25, 26		

through which the highly accurate VRT spectroscopy measurements can be analyzed in terms of an anisotropic multidimensional potential surface without significant loss in the quality of information. Generally, this implies that the various dynamical simplifications that are usually invoked to interpret the measurements of intermolecular properties (adiabatic approximations, distortion methods, etc.) out of mathematical necessity, must be avoided, or at least employed only with careful scrutiny. Fortunately, the recent experimental advances have been paralleled by similarly dramatic theoretical progress in our ability to address the dynamics of multidimensional systems. The discrete variable representation (DVR) (32), the pseudospectral method (33), and collocation method (34) are among the most powerful of these new dynamics methods. When coupled with the enhanced computational capability now available with the current generation of supercomputers, this scenario represents a truly revolutionary advance in our ability to address both intermolecular forces and the multidimensional intermolecular dynamics associated with them.

In this review, we describe an approach for directly determining multidimensional intermolecular potential energy surfaces from VRT spectra of binary van der Waals complexes measured with tunable far-IR lasers. This is by no means the only way to approach the potential inversion problem, and it may not be the best. It is, however, quite general and possesses a compelling degree of computational simplicity. Moreover, this same formalism is equally well adapted for analysis of mid-IR, microwave, or stimulated emission pumping spectra of weakly bound complexes. As such, it should be useful to a reasonably large audience.

COORDINATE SYSTEMS AND HAMILTONIANS: THE PSEUDODIATOMIC APPROACH

As the starting point of a general formalism for treating VRT spectra of a pair of interacting molecules, we make the central assumption that the

interacting monomers are not significantly affected by the weak van der Waals forces. The properties of the binary complex (e.g. dipole moment, electric field gradient, magnetic dipole moment) are then given simply by the projections of the relevant monomer properties onto the principal inertial axes of the complex. These are then easily corrected for the small (ca. 1%) polarization effects that accompany weak bond formation (35).

The canonical view of molecular structure in terms of a single deep minimum in the electronic potential energy surface, and the associated embedding of space- and body-fixed coordinate systems through the Eckhart conditions (36), is entirely abandoned in this description. Instead, we describe the complex in the language of scattering theory, viz. in terms of large amplitude dynamics of a set of Jacobi coordinates over a multidimensional IPS, which has a complicated topology (multiple minima and barriers). The set of generalized Jacobi coordinates appropriate for a complete description of the dynamics of a general complex, composed of two interacting polyatomic fragments, consists of five angles and a single distance (Figure 1). The **R** vector joins the centers of mass of the two interacting monomers, pointing from molecule A toward molecule B, and defines the weak bond axis; θ_A and θ_B are the angles between **R** and an appropriate symmetry axis in each monomer, ϕ_A and ϕ_B describe rotation

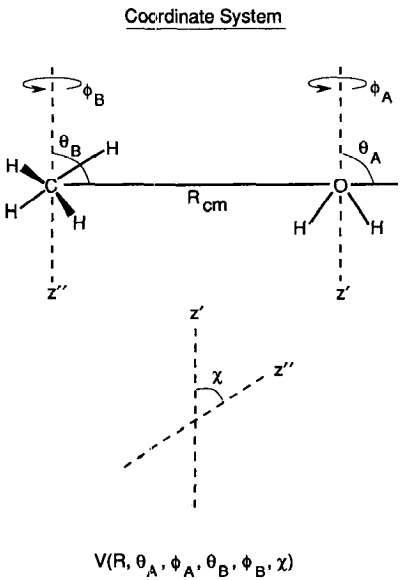

Figure 1 The Jacobi coordinate system for the intermolecular degrees of freedom of a polyatom-polyatom complex.

of each monomer about these symmetry axes, and $\chi = \chi_A - \chi_B$ is the dihedral angle between them. Thus, to describe the large amplitude dynamics of an arbitrary binary complex, one must solve a coupled six-dimensional problem in this set of internal coordinates, which is a formidable task by any standard.

The end-over-end rotation of the entire complex would normally (36) be described by a set of three Euler angles (α, β, γ), defined with respect to a space-fixed axis system (X, Y, Z). In the pseudodiatomic approach, the complex is instead viewed as a diatomic molecule, with the respective monomer masses M_1 and M_2 concentrated at the center-of-mass positions along the **R** vector. The end-over-end rotation can then be described by only two Euler angles, with the third set equal to zero.

Brocks et al (37) have used this pseudodiatomic embedding approach to derive the Hamiltonian for a general binary complex in body-fixed coordinates, thereby circumventing the complications in this procedure that are well known to scattering theorists and spectroscopists. They choose the **R** vector as the body-fixed z axis, and define a set of angular momentum operators:

$$J = j + l$$

$$j = j_A + j_B. \qquad 1.$$

Here, l is the end-over-end rotation of the pseudodiatom, j_A and j_B are the angular momenta of the individual polyatomic fragments A and B, and J is the total angular momentum. With the two-angle embedding approach, the commutation properties of J in body-fixed coordinates are not the usual ones (space-fixed or body-fixed); hence, J is termed a pseudoangular momentum operator. As a result of this complication, standard angular momentum results cannot be used without special considerations when a pseudodiatomic embedding procedure is used. This presents no additional complications, however, when a suitably chosen basis is used.

The Hamiltonian for a general binary complex can be expressed as (37)

$$\mathrm{H} = \mathrm{H}_A + \mathrm{H}_B + K_{INT} + V_{INT}, \qquad 2.$$

where the Hamiltonians for the individual nontunneling polyatomic fragments (H_A and H_B) are assumed to be separable from the kinetic and potential energy operators for the complex (K_{INT} and V_{INT}). Because the vibrational frequencies of the chemical bonds in the monomers are generally one to two orders of magnitude higher than is typical for van der Waals bonds, averaging the total Hamiltonian (2) over the high frequency motions is a good approximation. One thus obtains an effective Hamiltonian for each individual monomer vibrational state. The effective mono-

mer Hamiltonians, H_A and H_B, then assume the usual Watson form (36), by employing vibrationally averaged rotational constants and using components of angular momentum operators defined in their respective principal axis systems. The orientations of the monomers with respect to the body-fixed pseudodiatomic frame are given by two sets of Euler angles ω_A and ω_B, which include the angles $\theta_{A,B}$, $\phi_{A,B}$, and $\chi_{A,B}$ described above. The interaction potential depends on only five of these six angles, as only the relative orientation of the fragments must be specified.

The internal kinetic energy operator is

$$\hat{K}_{INT} = -\frac{\hbar^2}{2\mu \mathbf{R}^2}\frac{\partial}{\partial \mathbf{R}}\mathbf{R}^2\frac{\partial}{\partial \mathbf{R}} + \frac{1}{2\mu \mathbf{R}^2}[\hat{J}^2+\hat{j}^2-2\hat{j}\cdot\hat{J}]. \quad 3.$$

Brocks et al (37) define the operators $\hat{J}$ and $\hat{j}$. The first term in Equation 3 describes the vibrational motion along the van der Waals bond; the second characterizes the pseudodiatomic rotation and the Coriolis interactions.

The potential energy operator (V_{INT}) for the interacting fragments is actually the IPS that we seek to extract from the VRT data. The IPS is averaged over the monomer vibrational states and can be expressed in various forms. For molecules containing at least several heavy atoms, it is quite common to expand the potential as a sum of attractive and repulsive contributions between individual atoms within the complex. Such site-site potentials have been used in comparison of equilibrium structures of strongly anisotropic systems with the geometry of the potential minimum (38), but have not actually been used to fit spectroscopic data. A more useful approach for our purposes is to expand the IPS in a series of Wigner rotation matrices, expressed in the body-fixed Euler angles ω_A and ω_B. For a general binary cluster this becomes (37)

$$V^{INT}(R,\omega_A,\omega_B) = \sum_{\substack{L_A,K_A \\ L_B,K_B,L}} V_{L_A,K_A,L_B,K_B,L}(R)A_{L_A,K_A,L_B,K_B,L}(\omega_A,\omega_B).$$

$$A_{L_A,K_A,L_B,K_B,L}(\omega_A,\omega_B) = 8\pi^2(2L+1)^{1/2}$$

$$\times \sum_{M_A}\begin{pmatrix} L_A & L_B & L \\ M_A & -M_A & 0\end{pmatrix} D^{L_A*}_{M_A K_A}(\chi_A,\theta_A,\phi_A)D^{L_B*}_{M_A K_A}(\chi_B,\theta_B,\phi_B), \quad 4.$$

where the functions $D^{L*}_{MK}(\omega)$ are normalized Wigner D-matrices and $(\ldots)$ is a $3-j$ symbol. This form of the potential operator reflects the special nature of the weak bond and allows for several approximations that take advantage of the well-known properties of integrals over products of

Wigner D-matrices. The indices K_A and K_B range from $-L_A$ to L_A and $-L_B$ to L_B, respectively. The index L is the vector sum of L_A and L_B.

The values of the indices L and K and the relative contributions of different terms in the expansion are subject to symmetry constraints: For all molecules, L_A+L_B+L = even number (39); for electrostatic interactions expressed as a multipole expansion, $L = L_A+L_B$; and for molecules with a C_n axis, only values for which $K \bmod(n) = 0$ are nonzero. This expansion reduces to atom-polyatom and atom-diatom expressions when $L_B = 0$, and has been used in slightly modified forms in direct fits of a parameterized IPS to spectroscopic data for $Rg-H_2$ (40), $-HX$ (41–45), $-H_2O$ (46), and $-NH_3$ (21) complexes, as well as for CH_4-H_2O (30) and $(HF)_2$ (47). Several different formulations of these potential functions are commonly used, including expansions in spherical harmonics and Legendre polynomials for atom-molecule interactions. Functions are often used with normalization appropriate to the function with one more or one less degree of freedom to facilitate comparison between different complexes. Care must be taken that proper scaling for normalization has been considered when comparing the coefficients $V(R)$ from different treatments.

To derive physical insight into the forces that give rise to the IPS, it is useful to express the interaction potential as the sum of four anisotropic terms

$$\begin{aligned} V(R,\theta_A,\phi_A,\theta_B,\phi_B,\chi) &= V_{\text{electrostatic}}(R,\theta_A,\phi_A,\theta_B,\phi_B,\chi) \\ &+ V_{\text{induction}}(R,\theta_A,\phi_A,\theta_B,\phi_B,\chi) + V_{\text{dispersion}}(R,\theta_A,\phi_A,\theta_B,\phi_B,\chi) \\ &+ V_{\text{repulsion}}(R,\theta_A,\phi_A,\theta_B,\phi,\chi), \end{aligned} \quad 5.$$

and to expand each of these terms in a series of orthogonal polynomials, as in Equation 4. Functional forms for the expansion coefficients $V(R)$ (radial strength functions) are available for the electrostatic interaction and the induction forces, which involve dipole-dipole polarizabilities (α_{ij}) and dipole-quadrupole polarizabilities (A_{ijk}) (48). We reproduce the low-order equations here, arranged in the form of Equation 4.

$$V^{\alpha}_{\text{induction}} = \sum_{\substack{L_A,L_B,L \\ K_A,K_B}} \sum_{\ell'_A,\ell''_A} -\frac{1}{6}(4\pi)^{5/2}$$

$$\times \left[\frac{(\ell'_A+1)(\ell''_A+1)(2\ell'_A+3)(2\ell''_A+3)(2L_A+1)(2L_B+1)}{2L+1}\right]^{1/2}$$

$$\times C(\ell'_A+1\ell''_A+1\ell;000) \begin{Bmatrix} \ell'_A & 1 & \ell'_A+1 \\ \ell''_A & 1 & \ell''_A+1 \\ L_A & L_A & L \end{Bmatrix}$$

$$\times r^{-(\ell'_A+\ell''_A+4)}\alpha_{11}(L_BK_B)$$

$$\times \sum_{K'_AK''_A} C(\ell'_A\ell''_A\ell_A; K'_AK''_AK_A)Q\ell'_Ak'_AQ\ell''_Ak''_AA_{L_AK_AL_BK_BL}(\omega_A, \omega_B). \quad 6.$$

In Equation 6, $C(\ldots;\ldots)$ is a Clebsch-Gordon coefficient, and the quantity in brackets $\{\ \}$ is a $9-j$ symbol. For the induction energy associated with the charge distribution of molecule B and polarizability of molecule A, the subscripts A, B are interchanged:

$$V_{\text{electrostatic}} = \sum_{\substack{L_A,L_B \\ k_A,K_B,L}} (-1)^{L_A}\left[\frac{(2L)!}{(2L_A+1)!(2L_B+1)!}\right]^{1/2}$$

$$\times Q_{L_AK_A}Q_{L_BK_B}R^{-(L+1)}A_{L_AK_AL_BK_BL}(\omega_A, \omega_B) \quad 7.$$

$$V_{\text{dispersion}} = \sum_{\substack{L_A,L_B,L \\ K_A,K_B}} \frac{C_n^{L_AK_AL_BK_BL}}{R^n} A_{L_AK_AL_BK_BL}(\omega_A, \omega_B). \quad 8.$$

The molecular multipole moments, Q_{LM}, and static polarizabilities, $\alpha_{\lambda\mu}^{LM}$, used in these equations are expressed in irreducible spherical tensor form. Table 2 provides the low-order constants, defined in terms of Cartesian components with a normalization consistent with Equation 4. Exact calculation of the dispersion coefficients requires knowledge of the frequency-dependent polarizabilities. C_6 constants are available from dipole oscillator strength distributions for some systems, or they may be estimated, as Buckingham et al (1) discuss. Higher-order isotropic dispersion constants have been estimated by using static polarizabilities (42–44, 46) and calculated by ab initio theory (49).

By using these expressions and the molecular constants (dipole and

Table 2 Transformation from Cartesian to spherical multipole moments and polarizabilities

$Q_{00} = q$	$Q_{22} = \sqrt{\frac{1}{6}}(\theta_{xx}-\theta_{yy}+2i\theta_{xy})$
$Q_{10} = \mu_z$	$Q_{L-M} = (-1)^M Q^*_{LM}$
$Q_{11} = -\sqrt{2}(\mu_x+i\mu_y)$	$\alpha_{11}(00) = -\frac{1}{2}\left(\frac{3}{4\pi}\right)\frac{1}{\sqrt{3}}(\alpha_{xx}+\alpha_{yy}+\alpha_{zz})$
$Q_{20} = \theta_{zz}$	$\alpha_{11}(20) = \frac{1}{2}\left(\frac{3}{4\pi}\right)\frac{2}{\sqrt{3}}\left(\alpha_{zz}-\frac{1}{2}(\alpha_{xx}+\alpha_{yy})\right)$
$Q_{21} = -\sqrt{\frac{2}{3}}(\theta_{xz}+i\theta_{yz})$	

quadrupole moments, polarizabilities, etc.) obtained from either experiment or ab initio theory, it is possible to fix some of the leading contributions to the attractive portion of the IPS and then explore the contribution of the repulsive forces and higher-order attractive interactions. Intermolecular repulsion resulting from the overlap of electronic wavefunctions on different species rises exponentially at short range. As discussed by Buckingham et al (1), single-center expansions converge very slowly to true molecular shapes. It is better to expand the repulsive interaction as

$$A_{\text{repulsion}}(\omega_A, \omega_B)\, e^{-\beta(\omega_A,\omega_B)[R - R_m(\omega_A,\omega_B)]} \qquad 9.$$

where the functions $A_{\text{repulsion}}(\omega_A, \omega_B)$, $\beta(\omega_A, \omega_B)$, and $R_m(\omega_A, \omega_B)$ are separately expanded in a series of orthogonal polynomials. Anisotropy in $A_{\text{repulsion}}$ and R_m are important at the low energies sampled by the bound states; anisotropy in β is well known from molecular beam scattering results, but has not yet been shown to be important in the bound region of a van der Waals potential.

MULTIDIMENSIONAL DYNAMICS: COMPUTATIONAL STRATEGIES

Exact Methods

Having expressed the Hamiltonian that describes the vibrations, hindered rotations, and overall rotation of the complex in an appropriate form, we then compute the bound states for the problem by solving the Schrodinger equation. The problem of solving a set of coupled, multidimensional differential equations has recently received considerable attention. We note, in particular, the recent review by Bačić & Light (50). The most successful new methods employ a mixed basis set/pointwise approach. The power of these methods derives from their capabilities to obtain the eigenvalues and eigenvectors of the Hamiltonian accurately, without requiring that multidimensional integrals be computed to determine the matrix elements. Only the value of the IPS and the basis set on a grid of points is required. This effects a considerable savings in the time required to generate the eigenvalues of the Hamiltonian and in the complexity of the computational procedure.

Several pointwise methods have been implemented in the solution of the Schrodinger equation for molecular systems. Friesner and coworkers (33) have developed the pseudospectral method, principally in connection with the electronic structure problem. This approach is related to, but varies slightly from, the two methods that have been more extensively applied to the problem of heavy particle dynamics on an IPS with many strongly

coupled degrees of freedom. These two methods are the DVR, which has been developed by Light and coworkers (32), and the collocation method, which has generated a renewed interest for chemical applications since the recent work of Peet & Yang (34, 51–54). In the DVR, one solves the Schrodinger equation by expanding the wavefunction as a direct product of an orthonormal basis set in each coordinate. The basis is then related by a unitary transformation to one in which the coordinate operators are diagonal. For example, the effect of the operator $\hat{R}$ on the DVR function $|\Phi_i(R)\rangle$ is to generate the eigenvalue R_i, which is a point in the configuration space of the problem:

$$\hat{R}\Phi_i(R)\rangle = R_i|\Phi_i(R)\rangle. \qquad 10.$$

One then makes the approximation that the integrals over the IPS can be evaluated by quadrature on the DVR points, which results in a diagonal form for the matrix representation of the IPS. The Hamiltonian matrix in this formulation is sparse, because the only off-diagonal coupling terms result from the kinetic energy operators. The DVR has been applied to the study of highly excited vibrational levels of covalently bound species (H_2O, HCN) (55, 56) and to the calculation of energies for two-dimensional van der Waals systems, e.g. Ar-HCl (57) and Ar-HCN (58). The DVR is advantageous because the Hamiltonian matrix is symmetric, and small subspaces of the matrix may be evaluated in a recursive procedure of diagonalization and truncation. This allows for accurate evaluation of the eigenvalues of a large matrix by diagonalization of a series of smaller matrices, which translates into considerable computational savings, as the computer time is roughly proportional to the cube of the matrix dimension. The DVR method suffers from one major drawback, however, especially for application to weakly bound complexes that contain polyatomic molecules: A strict requirement for the implementation of a DVR is that the basis set be expressed as a direct product of functions in each coordinate. Basis functions that are the most natural choice for nonlinear systems, which exhibit large amplitude hindered rotation, viz. spherical harmonics or Wigner D-matrices, are compound functions spanning two or three coordinates, respectively, for which a direct product is not defined. For such problems, the collocation method is more efficient.

The collocation method has been applied to solution of one-, two-, and three-dimensional problems. Yang & Peet (34) studied the convergence of the method when it is applied to solve for the energies of a Morse oscillator. They then showed that the method could be applied to the solution of the Hamiltonian for the rotating Ar-HCl problem (51, 52), and they used a nondirect product basis to evaluate the eigenvalues of Ar-CO_2 (54). While addressing these two-dimensional systems, they also described an iterative

method for solving the large matrix eigenvalue problem represented by the multidimensional collocation equations. The collocation method is considerably simpler and more transparent than the DVR, but it also has some deficiencies. The collocation matrix equation appears in the form of a generalized unsymmetric eigenvalue problem. Formally, complex and spurious eigenvalues and nonorthogonal eigenvectors may arise from such a matrix, although in our experience, such results actually represent inadequate convergence of the basis set or the points and are easily recognized and circumvented by simply increasing the number of basis functions and points.

In essence, the collocation method amounts to an n-point quadrature approximation to the Rayleigh-Ritz variational method for solving the Schrodinger equation. The procedure for applying the collocation method is to expand a trial wavefunction as a linear combination of n basis functions. These functions are then considered an exact solution of the Schrodinger equation at n collocation points. The points are chosen to be an appropriate set of quadrature points in the configuration space of the problem. The resulting n coupled equations then appear in the form of a generalized eigenvalue problem:

$$\{\mathbf{H}-\mathbf{E}\Psi\}\mathbf{c}=0. \tag{11.}$$

Here, $\mathbf{H}$ is a matrix with elements H_{ji} given by $H|\Psi_i\rangle$ evaluated at the collocation point j, and Ψ is a matrix with column vectors $|\Psi_i\rangle$ evaluated at the collocation point j, and Ψ is a matrix with column vectors $|\Psi_i\rangle$ evaluated at the same set of points. The label i ranges from 1 to n, the number of basis functions in the trial wavefunction. The label j spans the same range, but identifies the point in configuration space at which the matrix element has been evaluated. Standard eigenvalue routines which return eigenvalues ($\mathbf{E}$) and the matrix of eigenvectors ($\mathbf{c}$), are available in the common mathematical libraries for solving the unsymmetrical matrix equation.

We begin implementation of the numerical procedures by expanding the wavefunction as a product of angular and radial functions:

$$\psi^J(\alpha,\beta,R,\theta_A,\phi_A,\theta_B,\phi_B,\chi)=\sum_{\Omega=-J}^{J}\sum_{j=|\Omega|}^{j^{\max}}\sum_{j_A=0}^{j_A^{\max}}$$

$$\times\sum_{k_A=j_A}^{j_A}\sum_{j_B=0}^{j_B^{\max}}\sum_{k_B=-j_B}^{j_B}\sum_{i=1}^{N_R}\sum_{\Omega_A\Omega_B}\frac{1}{R}\chi_i(R)\frac{(-1)^{j_A-j_B-\Omega}}{\sqrt{2j+1}}$$

$$\times\begin{pmatrix}j_A & j_B & j\\ \Omega_A & \Omega_B & \Omega\end{pmatrix}D^{j_A^*}_{\Omega_A k_A}(\chi,\theta_A,\phi_A)D^{j_B^*}_{\Omega_B k_B}(0,\theta_B,\phi_B)D^{J^*}_{M\Omega}(\gamma,\beta,\alpha). \tag{12.}$$

The angular functions are chosen to be products of Wigner D-matrices for the monomers A and B and for the overall pseudodiatomic rotation, to utilize the general results of Brocks et al (37). The radial functions $\chi_n(R)$ can be considered a set of distributed gaussians, or a set of orthonormal functions that represent the bound and unbound solutions to a suitable model one-dimensional problem. These primitive functions are then symmetrized to transform according to the irreducible representations (Γ) of the molecular symmetry group for the complex. The Hamiltonian does not mix functions of different symmetry or total angular momentum.

We then operate on the symmetrized wavefunction with the Hamiltonian, multiply on the left by the complex conjugate of the spatial wavefunction, and integrate over α, β, γ to reduce the problem to one that involves only the internal coordinates. This gives the set of coupled differential equations, which we solve by collocation. Cohen & Saykally (46) describe this procedure in detail for the specific case of an atom-polyatom complex.

The next step in application of the collocation method is to choose a set of n quadrature points, one corresponding to each basis function. Because symmetry operations have been applied to reduce the size of the Hamiltonian matrices, the range at which the points are chosen must also be appropriately reduced. The points should be chosen from the smallest interval of configuration space, which is mapped onto the rest of the configuration space by successive symmetry operations. In Ar-H_2O, for example, this symmetry occurs in the ϕ coordinate, which represents the angle of internal rotation about the C_{2v} axis, for which the interval $0 \leq \phi \leq \pi/2$ is mapped onto the range $0-2\pi$, by symmetry operations of the molecular symmetry group. The choice of collocation points is discussed in more detail in references 46, 52, and 59.

Once the collocation points are chosen, the coupled equations are evaluated on the grid of collocation points, and the resulting matrix is diagonalized by standard numerical methods. The results obtained by using collocation are not variational, in the sense of a strict upper bound to the eigenvalues that would be obtained with an infinite basis set. They are, however, an approximation for the results that would be obtained in a variational calculation with accuracy of a numerical quadrature on the collocation points. Peet & Yang (34, 51–54) showed the rate of convergence to be roughly exponential for some one- and two-dimensional problems. The absolute level of convergence depends on the details of the particular system in question, including the reduced mass, the monomer rotational constants, and the magnitude of the anisotropy. The most strongly bound states, which are usually the ones accessed spectroscopically, are more easily converged than highly excited levels. In fits to experimental data,

one attempts to reproduce vibrational frequencies and rotational spacings to about 1 part in 10^3–10^4. Thus, the calculated eigenvalues must be converged to at least this level of accuracy.

The first step in a fit of experimental data to the IPS is to choose an appropriate set of unknowns to vary in the potential expansion of Equation 5. A typical (40, 42, 46) procedure is to fix all the molecular constants required to calculate the attractive forces through the nth power of R at known values and then to lump all of the attractive terms of higher order into a single expansion that varies as the $n+1$ power of R:

$$V_{\text{ATTRACTIVE}} = V_{\text{FIX}} + C_{n+1}(\omega_A, \omega_B) R^{-n+1}. \quad 13.$$

This reduces the number of unknown parameters substantially. To reduce the parameter space further, the well depth $\varepsilon(R_m; \omega_A, \omega_B)$ is typically expanded at the position of the radial minimum $R_m(\omega_A, \omega_B)$ for each angular configuration in a series of orthogonal polynomials. The coefficients $A_{\text{repulsion}}(\omega_A, \omega_B)$ and $C_{n+1}(\omega_A, \omega_B)$ are then determined by requiring that

$$V(R_m, \omega_A, \omega_B) = -\varepsilon(R_m, \omega_A, \omega_B), \quad 14.$$

and

$$V'(R_m, \omega_A, \omega_B) = 0, \quad 15.$$

where the prime indicates the first derivative with respect to R. This procedure, first employed by Hutson and LeRoy in fits to Rg–H_2 spectra, reduces the number of parameters, as both $A_{\text{repulsion}}(\omega_A, \omega_B)$ and $C_{n+1}(\omega_A, \omega_B)$ are determined by fitting $\varepsilon(\omega_A, \omega_B)$. It also focuses attention on the region of the IPS that is sampled most extensively by the spectroscopic data, viz. the region surrounding the potential minimum.

The numerical procedures outlined in this section have been implemented in determination of the IPS of ArH_2O (46). The well depth $\varepsilon(\theta, \phi)$, the position of the radial minimum $R_m(\theta, \phi)$, and the repulsive exponent $\beta(\theta, \phi)$ were expanded in a series of symmetry adapted renormalized spherical harmonics, rather than the Wigner D matrices of Equation 5. In our initial study, nine potential parameters, including ε_{00}, ε_{10}, ε_{20}, ε_{22}, R^m_{00}, R^m_{10}, R^m_{20}, R^m_{22}, and β_{00}, were allowed to vary in a fit to an experimental data set, which consisted of four VRT band origins and seven rotational term values. Higher order anisotropies in ε, R^m, and β were fixed at zero. Contours of the resulting IPS, denoted AW1, are shown in Figures 2 and 3.

The eigenvalues of the Hamiltonian were obtained by using a basis set of 11 radial functions and 10–15 angular functions, depending on the symmetry of the subblock, for $J = 0$. The $J = 1$ eigenvalues required $(2J+1)$

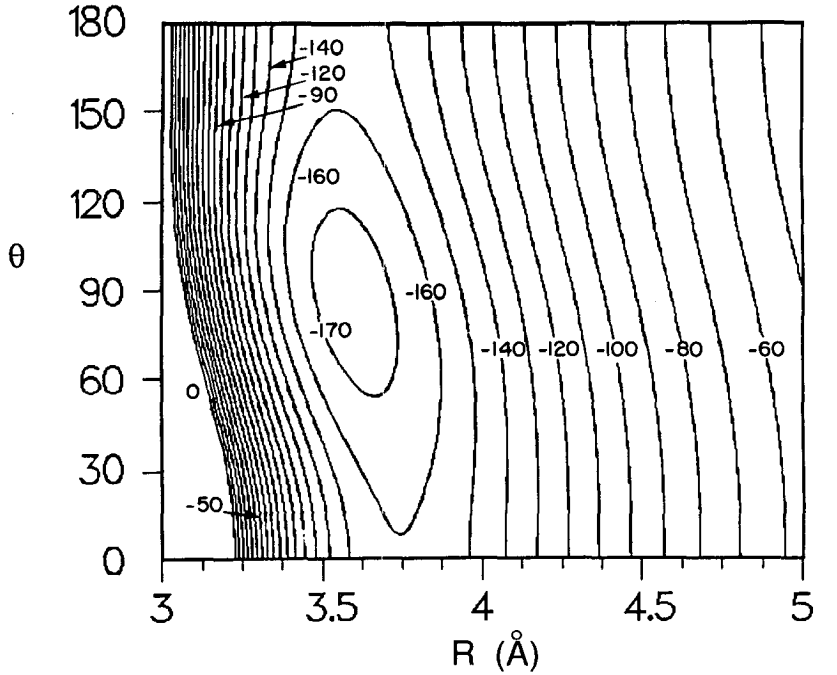

Figure 2 A cut through the AW1 intermolecular potential surface of Ar–H_2O with $\phi = 0$. All four atoms are coplanar, R is the center of mass separation, and θ is the angle between the H_2O C_{2v} axis and the R vector. The hydrogen atoms point toward the argon at $\theta = 0°$ and away at $\theta = 180°$.

more angular functions. This basis gave convergence of 0.02 cm^{-1} for the intermolecular vibrational frequencies used in the fit and 0.0001 cm^{-1} for rotational term values. Three of the four possible symmetries were required to calculate all of the observed frequencies. Each call to the eigenvalue subroutine required two minutes of central processing unit (CPU) time on a CRAY-XMP/14. For nine parameters, each least squares iteration required about 20 minutes. Approximately ten hours of CPU time were used to obtain a converged fit.

Approximate Methods

The details given above for the exact atom-polyatom calculation illustrate the level of computational effort required to properly analyze VRT spectra of a three-dimensional system. Extension to systems with more degrees of freedom clearly requires much more effort (computation time increases ~1000-fold with each added degree of freedom). Therefore, approximate methods must be employed, at least with present technology. Moreover,

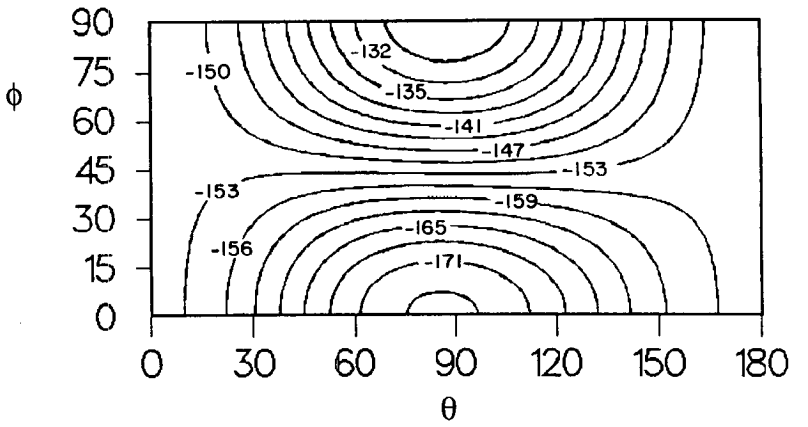

Figure 3 A cut through the AW1 surface at Ar–H_2O at $R = 3.65$ Å. The ϕ coordinate specifies rotation of the H_2O about its C_{2v} axis. The other coordinates are discussed in Figure 2 and the text.

although the use of the collocation method, or another suitable computational approach for obtaining the exact eigenvalues and eigenvectors for the full multidimensional problem, is essential for extracting a quantitatively accurate IPS, approximate treatments of the dynamics can actually offer deeper insight into the relationship between anisotropy in the IPS and the experimental observables. The most revealing approximations are those that are based on approximate separability of the internal coordinates, particularly the reversed adiabatic approximation (RAA), which Hutson (60–62) discusses extensively. In this treatment, the angular and radial motions are presumably separable. To the extent that this assumption holds (severe breakdown of this approximation is not unusual), a family of bending levels associated with the same stretching state (usually the ground state) may be associated with the same effective angular potential surface.

To calculate the VRT spectrum of a polyatom-polyatom cluster within the reversed adiabatic approximation, one begins with expansion of the wavefunction, as in Equation 12. This form of the wavefunction is most appropriate if the internal rotation in both monomers is strongly coupled to the molecular frame. If one or both angular momenta are more nearly coupled to the space fixed frame, or if they are coupled to each other, alternative basis sets may give a better first-order description of the intermolecular dynamics, in analogy to the different coupling cases described by Hutson (60–62) for atom-diatom complexes. The effects of the kinetic energy operators in the Hamiltonian (Equation 3) on this basis are given in Table 3. The matrix elements of the potential are (37)

Table 3 Effect of the Hamiltonian operators on the components of the primitive basis set

$\hat{J}^2 D^{J*}_{M,\Omega}(\alpha,\beta,0) = J(J+1)D^{J*}_{M,\Omega}(\alpha,\beta,0)$	$\hat{j}_\pm^{m^2} D^{j*}_{\Omega,k}(\gamma,\theta,\phi) = F^{\pm}_{j,k} D^{j*}_{\Omega,k\pm2}(\gamma,\theta,\phi)$
$\hat{j}^{m^2} D^{j*}_{\Omega,k}(\gamma,\theta,\phi) = j(j+1)D^{j*}_{\Omega,k}(\gamma,\theta,\phi)$	$\hat{j}^2 D^{j*}_{\Omega,k}(\gamma,\theta,\phi) = j(j+1)D^{j*}_{\Omega,k\pm2}(\gamma,\theta,\phi)$
$\hat{J}_\pm D^{J*}_{M,\Omega}(\alpha,\beta,0) = C^{\pm}_{J,\Omega} D^{J*}_{M,\Omega\pm1}(\alpha,\beta,0)$	$C^{\pm}_{j,\Omega} = [j(j+1)-\Omega(\Omega\pm1)]^{1/2}$
$\hat{j}_z^{m^2} D^{j*}_{\Omega,k}(\gamma,\theta,\phi) = k^2 D^{j*}_{\Omega,k}(\gamma,\theta,\phi)$	$F^{\pm}_{j,k} = [j(j+1)-k(k\pm1)]^{1/2}[j(j+1)-(k\pm1)(k\pm2)]^{1/2}$
$\hat{j}_\pm D^{j*}_{\Omega,k}(\gamma,\theta,\phi) = C^{\pm}_{j,\Omega} D^{j*}_{\Omega\pm1,k}(\gamma,\theta,\phi)$	

$$\langle j'_A, k'_A j'_B j' \Omega' | V_{INT} | j_A, k_A j_B, k_B j \Omega \rangle = \delta_{\Omega'\Omega} \sum_{\substack{L_A,K_A \\ L_B,K_B,L}} V_{L_A,K_A,L_B,K_B,L}(R) \times g_{L_A,K_A,L_B,K_B,L}(j'_A, j'_B j'; j_A, j_B j; k_A, k'_B k'_A, k_B; \Omega)$$

$$g = (-1)^{j'+j'_A+j'_B+L_A+L_B-k'_A-k'_B-\Omega} \times [(2j'_A+1)(2j_A+1)(2L'_A+1)(2j'_B+1)(2j_B+1)(2L_B+1)$$
$$\times (2j'+1)(2j+1)(2L+1)]^{1/2} \begin{pmatrix} j'_A & L_A & j_A \\ k'_A & K_A & k_A \end{pmatrix} \times \begin{pmatrix} j'_B & L_B & j_B \\ k'_B & K_B & k_B \end{pmatrix} \begin{pmatrix} j' & L & j \\ -\Omega & 0 & \Omega \end{pmatrix} \begin{Bmatrix} j'_A & J_A & L_A \\ j'_B & j_B & L_B \\ j' & j & L \end{Bmatrix}. \quad 16.$$

The role of the radial strength functions $V(R)$ in the expansion of the IPS is greatly simplified in the RAA, because the exact functional form is no longer necessary, and numerical values for the expectation values of the radial coefficients over the wavefunction of interest may be substituted. For instance, in his RAA analysis of the spectrum of Ar-H_2O (62), Hutson showed that the vibrational energies of the first two Σ bending levels of ortho symmetry are given by the approximate expressions:

$$E(\Sigma_{1_{01}}) = V_{00} - \frac{1}{5}V_{20} + \frac{\sqrt{6}}{5}V_{22} + E_{1_{01}},$$

$$E(\Sigma_{1_{10}}) = V_{00} - \frac{1}{5}V_{20} - \frac{\sqrt{6}}{5}V_{22} + E_{1_{10}}, \quad 17.$$

if anisotropies involving terms of higher order than V_{22} are neglected. In the above expression, we omit the subscripts $L_B = K_B = 0$, because the

argon atom is spherical and the subscript $L = L_A$. $E_{1_{01}}$ and $E_{1_{10}}$ refer to the free rotor energies of water.

Often in the absence of experimental data, it is useful to consider either the effects on a spectrum when the anisotropies are varied over a range of reasonable values, or trends in the spectrum as the anisotropies are increased by taking the molecule from a near free internal rotor to a near rigid system. Correlation diagrams for various combinations of anisotropies have been presented for atom-diatom systems (41, 60, 61).

These matrix expressions may also be used to evaluate the pseudodiatomic rotational term values. This can serve two purposes: The values can be used to establish energy differences when direct spectroscopic measurements are not available and the RAA is believed to be appropriate. And, when the energy differences are well established, the rotational term values give some indication of the validity of the RAA. If we express the angular momentum operators of the Hamiltonian in the basis of Equation 16, then the rotational kinetic energy is given by a diagonal contribution

$$\frac{\hbar^2}{2\mu\mathbf{R}^2}[J(J+1)+j(j+1)-2\Omega^2]\delta_{\tau'\tau}\delta_{\Omega'\Omega}, \qquad 18.$$

and an off-diagonal Coriolis term

$$\frac{\hbar^2}{2\mu\mathbf{R}^2}[C^+_{j\Omega}C^+_{J\Omega}+C^-_{j\Omega}C^-_{J\Omega}]\delta_{\tau'\tau}\delta_{\Omega',\Omega\pm1}. \qquad 19.$$

Here, μ is the pseudodiatomic reduced mass, R is the coordinate operator, and τ refers to all quantum numbers other than the projection Ω and the radial quantum numbers n. Within the RAA, we assume that the $1/\mathbf{R}^2$ operator does not cause appreciable mixing of different radial functions, and equate $\hbar^2/\mu R^2$ with the rotational constant, B, in the two states that are mixed by the Coriolis interaction. B is then considered identical in all states that share the same effective radial IPS. In the symmetrized basis, the effect of the off-diagonal Coriolis operator is to mix states of the same total J and parity, which differ in the Ω quantum number by 1.

Consider states with total $J = 1$; only $\Omega = 0$ (Σ) and $\Omega = 1$ (Π) states are involved, and the existence of $\Omega = 2$, (Δ) states cannot yet complicate the picture. For a state having a wavefunction dominated by $j = 1$, the Coriolis matrix element reduces to $H_{Coriolis} = 2B[J(J+1)]^{1/2}$ and for $j = 2$, $H_{Coriolis} = 2\sqrt{3}B[J(J+1)]^{1/2}$. A 2×2 Hamiltonian matrix for the mixed Σ^+ and Π^+ states results,

$$\begin{bmatrix} H_\Sigma & H_{Coriolis} \\ H_{Coriolis} & H_\pi \end{bmatrix} \qquad 20.$$

and the unperturbed component of the Π state, which is of the opposite parity, has an energy given by

$$E_{\pi}^{-} = [H_{\pi}]. \qquad 21.$$

The 2×2 matrix may be diagonalized perturbatively, assuming that $(H_{Coriolis})^2 \ll H_{\Pi} - H_{\Sigma}$, with the results:

$$E_{\Sigma}^{+} = H_{\Sigma} - H_{Coriolis}^2/(H_{\Pi} - H_{\Sigma})$$

$$E_{\Pi}^{+} = H_{\Pi} + H_{Coriolis}^2/(H_{\Pi} - H_{\Sigma}). \qquad 22.$$

The simplest manifestation of this operator to consider is the ℓ-splitting of the two $J = 1$ levels in Π states. This splitting, which we denote $q\ell(J = 1)$, is approximately

$$E_{\Pi}^{+} - E_{\Pi}^{-} = 8B^2/(H_{\Pi} - H_{\Sigma}) \qquad 23.$$

in states with $j = 1$. The $+/-$ signs are used here solely to differentiate between the two components of the Π state and do not reflect any molecular symmetry. It is important to note that the Coriolis-induced shift in the rotational term value of $J = 1$ in the Σ level is equal and opposite to that in the Π state. Large fractional errors in the effective internuclear distance may be obtained if this effect is not explicitly accounted for in the analysis of states with substantial internal angular momentum.

This expression is remarkably accurate for the ortho $j = 1$ VRT states of Ar-H_2O (15, 16). The splitting in $\Pi(1_{01})$ is 0.205 GHz. Substituting into Equation 23, and using an average rotational constant of 3 GHz, which is within 2% of the experimental values (3.015, 2.951 GHz), yields an estimate of the energy difference between $J = 1$ in the $\Sigma(1_{01})$ level and $J = 1$ in the $\Pi(1_{01})$ state of 351 GHz. This compares with the experimental value of 340 GHz (15, 16, 63). In the $\Pi(1_{10})$ state, the observed splitting is 0.147 GHz, which yields an estimate of the spacing between $J = 1$, $\Sigma(1_{10})$ and $J = 1$, $\Pi(1_{10})$ of 489 GHz, compared with the experimental value of 452 GHz. The accuracy of these estimates is strong evidence that these VRT states of Ar-H_2O very nearly correspond to the pure basis functions used (17), and supports the idea that all of the states involved sample the same effective radial potential.

The results for the first para bending levels of Ar–H_2O are dramatically different (17). In the 1_{11} states, we measure $q\ell(J = 1)$ to be 0.251 GHz. By using this measured splitting, we estimate the energy spacing of $\Pi(1_{11})$-$\Sigma(1_{11})$ to be 286 GHz, more than twice the experimental spacing of 115 GHz. The failure of this simple model to account for the positions of the observed bands simultaneously with the observed spacings indicates strongly that there is significant mixing of the Σ and/or Π levels with other

nearby states. The exact three-dimensional calculations suggest that the predominant source of mixing occurs between $n = 1, \Sigma(0_{00})$ and $n = 0, \Sigma(1_{11})$, which implies that the RAA is not appropriate for analysis of these states. Similar effects of bend-stretch coupling are manifested in other excited states of Ar-H_2O, Ar-NH_3, and probably most other complexes. Hence, the RAA is not a generally applicable description for the VRT dynamics of complexes.

Other experimentally accessible properties, such as the dipole moment or nuclear quadrupole coupling constant, may also be evaluated within the RAA. The dipole moment of the complex may be approximated to be the projection of the dipole moments of the monomers, with corrections for induction effects. The expectation value of this property over the wavefunctions extracted from diagonalization of the above matrices can be obtained by analytic or numerical integration. The accuracy of the results depends on approximations used to estimate the expectation of value of R in the induction contributions, and again on the validity of the RAA approximation.

EXAMPLES

$ArNH_3$

The $ArNH_3$ complex was first studied in detail by Nelson et al (64), who suggested that this complex was unique among NH_3-containing complexes because the umbrella inversion motion was not quenched. Rigorous proof of this conjecture was obtained with the spectroscopic assignment of the inversion transitions in $ArNH_3$ by Zwart et al (22). Thus, the IPS of the complex is a four-dimensional function of R, θ, ϕ, and ρ—the inversion coordinate.

Schmuttenmaer et al (21) have developed an approximate angular IPS $V_{eff}(\theta, \phi)$ based on tunable far-IR laser VRT measurements of three bands of para Ar–NH_3. Two bands are reported by Schmuttenmaer et al (21), and one by Gwo et al (20). The electric dipole and nuclear quadrupole measurements of Nelson et al (64) were also included in the fit. The leading three anisotropic terms in the potential expansion were considered, and a range of reasonable potentials was developed. The data set was insufficient to establish the anisotropy in ϕ, and the potential was, therefore, constrained to be isotropic in this coordinate. Figure 4 illustrates three limiting potential surfaces, the bending energy levels, and the wavefunctions. The IPS for $ArNH_3$ is dominated by anisotropic repulsion, which favors a minimum with the C_{3v} axis nearly perpendicular to the van der Waals bond axis.

Additional measurements of the VRT spectrum of Ar–NH_3 have since

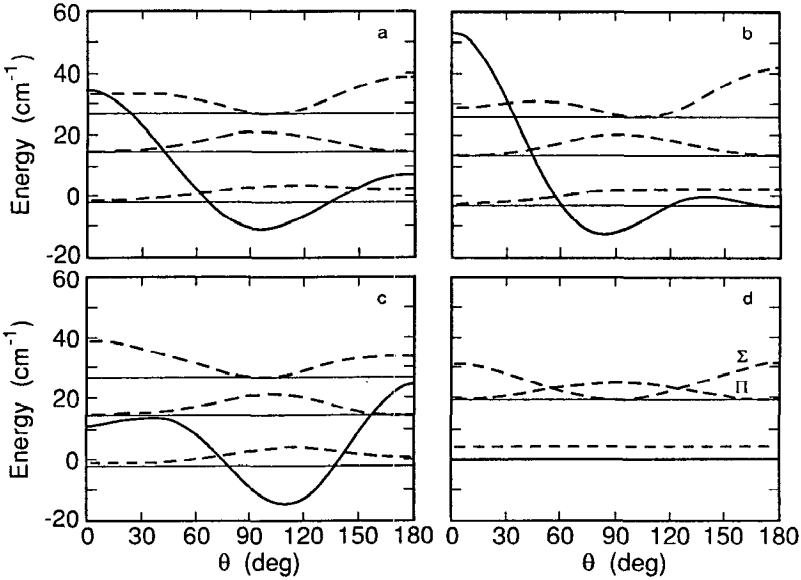

Figure 4 Potential energy surfaces (*heavy solid curves*), vibrational energy levels (*solid horizontal lines*), and the square amplitude of the wavefunctions (*dotted curves*) for Ar–NH_3. The best fit (V_{30} fixed at 3 cm^{-1}) is shown in (*a*), and fits with $V_{30} = \pm 15$ are shown in (*b*) and (*c*), respectively. All three are consistent with the experimental data. In (*d*), the results for an isotropic potential are shown for comparison.

been reported by Zwart et al (22). Schmuttenmaer et al (65) are currently developing a full four-dimensional surface, which will explicitly include the effects of anisotropy in the ϕ coordinate and angular radial coupling.

ArH_2O

The AW1 surface developed by Cohen & Saykally (46) has been tested by measurements of six new VRT bands (17, 63) and by the measurement of the dipole moment and quadrupole coupling constants of the ground vibrational levels by Fraser et al (66). These new measurements draw attention to the weaknesses of the AW1 parameterization. The dipole moment measurement requires a larger $|V_{10}|$ anisotropy in the region of the potential minimum than is present in the AW1 surface. This, in turn, requires other anisotropic terms, which were constrained to be equal to zero on the AW1 surface, to be included. The sign of V_{10} is not easily determined: It is not determined by vibrational splittings in Ar–H_2O, but only by isotope shifts and rotational term values.

The VRT measurements are more difficult to interpret than the dipole

moment. They demand a surface with significantly more angular-radial coupling than is present in the AW1 surface, but do not affect a single specific potential parameter. They also require inclusion of ε_{30}, ε_{32}, R^{m}_{30}, and R^{m}_{32} anisotropies. Initial fits to this new data set indicate that the isotropic well depth V_{00}, is close to 125 cm^{-1}, 30 cm^{-1} below the AW1 value [153.3 (4)]. This is more than 30 standard deviations from the previously determined value, but the well depth parameter, (V_{00}), was highly correlated (−0.98) with the repulsive wall parameter β_{00} in the AW1 fit. The current fits indicate that these two parameters are much less correlated (−0.94) and, thus, are expected to be more reliable. Cohen & Saykally (67) present a full analysis of the Ar–H_2O potential, and of data for Ar–D_2O.

CH_4-H_2O

The high symmetry of the CH_4-H_2O cluster makes it a relatively simple starting point for the investigation of weak interactions between two polyatomic molecules. Cohen et al (30) have measured and assigned six different VRT bands of this complex (30). These spectra were then compared with the bending values of two different effective angular IPSs calculated by using the RAA.

The potential energy surface was taken to be of the form of Equation 5, evaluated in a Jacobi coordinate system with the origin at the H_2O center of mass. The van der Waals bond length was fixed at the experimentally determined value of 3.720 Å. In both IPSs the electrostatic attraction through R^{-7} terms was fixed by using experimentally determined multipoles of H_2O and CH_4. In addition, anisotropic terms that involve only one subunit ($V_{L_AK_A00L}$, $V_{00L_BK_B}$) were fixed at the corresponding values for Ar–H_2O (46, 67) and Ar–CH_4 (68). These terms represent the sum of induction, dispersion, and repulsive forces. Eigenvalues were calculated on this IPS and on another that had a large anisotropic repulsive terms of the form $V_{L_AK_AL_BK_BL}$; $L_A, L_B \neq 0$. These terms were considered opposite in sign and one half the magnitude of the attractive anisotropies. (Neither surface has impressive agreement with the experimental data.) Measurement of many more VRT levels are necessary before the exact shape of the intermolecular potential for this interesting complex can be experimentally determined.

CONCLUSION

Advances in both experimental and computational methods offer the possibility for determining exact IPSs for binary van der Waals and hydrogen bonded clusters. These methods permit IPSs for any atom-molecule cluster

to be studied in extraordinary detail. Intermolecular dynamics and IPSs for clusters of higher dimensionality are currently a subject of active experimental interest, with sufficient data available to warrant development of experimental potentials for $(HF)_2$ (69a, 70), $(HCl)_2$ (23, 24, 71), $(H_2)_2$ (72), Ar_2HCl (31), HF–HCN (73), H_2–HF (74), and possibly $(H_2O)_2$ (25, 26) and $(NH_3)_2$ (27). Intermolecular potentials for all of these systems have been discussed in the literature (75–81), but only in the case of $(HF)_2$ (47) has an IPS actually been refined by fitting to VRT data. Detailed experimental characterization of the anisotropy of intermolecular forces in these and other systems can be expected in the near future.

ACKNOWLEDGMENTS

This work was supported by the National Science Foundation Grant #CHE86-12296 and by the Director, Office of Energy Research, Office of Basic Energy Sciences, Chemical Sciences Division of the US Department of Energy, under contract No. DE-AC03-76SF00098.

Literature Cited

1. Buckingham, A. D., Fowler, P. F., Hutson, J. M. 1988. *Chem. Rev.* 88: 963
2. Hutson, J. M. 1990. *Annu. Rev. Phys. Chem.* 41: 123
3. Novick, S., Leopold, K., Klemperer, W. 1989. In *Atomic and Molecular Clusters*, ed. E. Bernstein. New York: Elsevier
4. Nesbitt, D. J. 1988. *Chem. Rev.* 88: 843
5. Miller, R. E. 1988. *Science* 240: 447; Miller, R. E. 1986. *J. Phys. Chem.* 90: 3301
6. Lovejoy, C. M., Nesbitt, D. J. 1986. *J. Phys. Chem.* 90: 3301
7. Marshall, M. D., Charo, A., Leung, H. O., Klemperer, W. 1985. *J. Chem. Phys.* 83: 4924
8. Ray, D., Robinson, R. L., Gwo, D., Saykally, R. J. 1986. *J. Chem. Phys.* 84: 1171
9. Saykally, R. J. 1989. *Acc. Chem. Res.* 22: 295
10. Busarow, K. L., Blake, G. A., Laughlin, K. B., Cohen, R. C., Lee, Y. T., Saykally, R. J. 1988. *J. Chem. Phys.* 89: 1268
11. Blake, G. A., Laughlin, K. B., Cohen, R. C., Busarow, K. L., Gwo, D.-H., et al. 1991. *Rev. Sci. Inst.* In press
12. Blake, G. A., Laughlin, K. B., Cohen, R. C., Busarow, K. L., Gwo, D.-H., et al. 1991. *Rev. Sci. Inst.* In press
13. Cohen, R. C., Saykally, R. J. 1991. *J. Phys. Chem.* In preparation
14. Firth, D. W., Dvorak, M. A., Reeve, S. W., Ford, R. S., Leopold, K. R. 1990. *Chem. Phys. Lett.* 168: 161
15. Cohen, R. C., Busarow, K. L., Laughlin, K. B., Blake, G. A., Havenith, M., et al. 1988. *J. Chem. Phys.* 89: 4494
16. Cohen, R. C., Busarow, K. L., Lee, Y. T., Saykally, R. J. 1990. *J. Chem. Phys.* 92: 169
17. Cohen, R. C., Saykally, R. J. 1991. *J. Chem. Phys.* In preparation
18. Suzuki, S., Bumgarner, R. E., Stockman, P. A., Green, P. G., Blake, G. A. 1991. *J. Chem. Phys.* 94: 824
19. Zwart, E. 1990. PhD thesis. Univ. Nijmegen, The Netherlands
20. Gwo, D.-H., Havenith, M., Cohen, R. C., Busarow, K. L., Schmuttenmaer, C. A., et al. 1990. *Mol. Phys.* 71: 453
21. Schmuttenmaer, C. A., Cohen, R. C., Loeser, J., Saykally, R. J. 1991. *J. Chem. Phys.* In press
22. Zwart, E., Linnartz, H., Meerts, W. L., Fraser, G. T., Nelson, D. D. Jr., Klemperer, W. 1991. *J. Chem. Phys.* Submitted
23. Blake, G. A., Busarow, K. L., Cohen, R. C., Laughlin, K. B., Lee, Y. T., Saykally, R. J. 1988. *J. Chem. Phys.* 89: 6577

24. Blake, G. A., Bumgarner, R. E. 1989. *J. Chem. Phys.* 91: 7300
25. Busarow, K. L., Cohen, R. C., Blake, G. A., Laughlin, K. B., Lee, Y. T., Saykally, R. J. 1989. *J. Chem. Phys.* 90: 3937
26. Zwart, E., ter Meulen, J. J., Meerts, W. L. 1990. *Chem. Phys. Lett.* 166: 500
27. Havenith, M., Cohen, R. C., Gwo, D.-H., Busarow, K. L., Lee, Y. T., Saykally, R. J. 1991. *J. Chem. Phys.* 94: 4776
28. Bumgarner, R. E., Stockman, P. A., Green, P. G., Blake, G. A. 1991. *Chem. Phys. Lett.* 176: 123
29. Bumgarner, R. E., Bowen, J., Green, P. G., Blake, G. A. In preparation
30. Cohen, R. C., Schmuttenmaer, C. A., Busarow, K. L., Saykally, R. J. In preparation
31. Elrod, M. E., Steyert, D. W., Saykally, R. J. 1991. *J. Chem. Phys.* 94: 58
32. Light, J. C., Whitnell, R. M., Park, T. J., Choi, S. E. 1989. *Supercomputer Algorithms for Reactivity, Dynamics and Kinetics of Small Molecules*, ed. A. Lagana. *NATO ASI Ser. C*, 277: 187. Dordrecht: Kluwer
33. Ringnalda, M. N., Belhadj, M., Friesner, R. A. 1990. *J. Chem. Phys.* 93: 3397 and references therein
34. Yang, W., Peet, A. C. 1988. *Chem. Phys. Lett.* 153: 98
35. Novick, S. E., Davies, P., Harris, S. J., Klemperer, W. 1973. *J. Chem. Phys.* 59: 2273
36. Papousek, D., Aliev, M. R. 1982. *Molecular Vibrational-Rotational Spectra.* Amsterdam: Elsevier
37. Brocks, G., van der Avoird, A., Sutcliffe, B. T., Tennyson, J. 1983. *Mol. Phys.* 50: 1025
38. Buckingham, A. D., Fowler, P. W. 1983. *J. Chem. Phys.* 79: 6426
39. van der Avoird, A., Wormer, P. E. S., Muldur, F., Berns, R. M. 1980. *Top. Curr. Chem.* 93: 1
40. Leroy, R. J., Hutson, J. M. 1987. *J. Chem. Phys.* 86: 837
41. Hutson, J. M., Howard, B. J. 1982. *Mol. Phys.* 45: 769; 1981. *Mol. Phys.* 43: 493
42. Hutson, J. M. 1989. *J. Chem. Phys.* 89: 4550
43. Hutson, J. M. 1989. *J. Chem. Phys.* 91: 4455
44. Hutson, J. M. 1989. *J. Chem. Phys.* 91: 4448
45. Nesbitt, D. J., Child, M. S., Clary, D. C. 1989. *J. Chem. Phys.* 90: 4855
46. Cohen, R. C., Saykally, R. J. 1990. *J. Phys. Chem.* 94: 7991
47. Barton, A. E., Howard, B. J. 1982. *Faraday Discuss. Chem. Soc.* 73: 45
48. Gray, C. G., Gubbins, K. E. 1984. *Theory of Molecular Fluids: Vol. 1.* Oxford: Clarendon
49. Rijks, W., Wormer, P. E. S. 1989. *J. Chem. Phys.* 90: 6507; 1990. *J. Chem. Phys.* 92: 5754
50. Bačić, Z., Light, J. C. 1989. *Annu. Rev. Phys. Chem.* 40: 469
51. Peet, A. C., Yang, W. 1989. *J. Chem. Phys.* 90: 1746
52. Peet, A. C., Yang, W. 1989. *J. Chem. Phys.* 91: 6598
53. Yang, W., Peet, A. C., Miller, W. H. 1989. *J. Chem. Phys.* 91: 7537
54. Yang, W., Peet, A. C. 1990. *J. Chem. Phys.* 92: 522
55. Bačić, Z., Waff, O., Light, J. C. 1988. *J. Chem. Phys.* 89: 947
56. Bačić, Z., Light, J. C. 1987. *J. Chem. Phys.* 86: 1065
57. Choi, S. E., Light, J. C. 1990. *J. Chem. Phys.* 92: 2129
58. Mladenovic, M., Bačić, Z. 1991. *J. Chem. Phys.* 94: 4988
59. Friesner, R. A. 1988. *J. Phys. Chem.* 92: 3091
60. Hutson, J. M. 1991. *Advances in Molecular Vibrations and Collision Dynamics*, Vol. 1. In press
61. Dubernet, M., Flower, D., Hutson, J. M. 1991. *J. Chem. Phys.* In press
62. Hutson, J. M. 1990. *J. Chem. Phys.* 92: 157
63. Lascola, R., Nesbitt, D. J. 1991. *J. Chem. Phys.* Submitted
64. Nelson, D. O. Jr., Fraser, G. T., Peterson, K. I., Zhao, K., Klemperer, W., et al. 1986. *J. Chem. Phys.* 85: 5512
65. Schmuttenmaer, C. A., Cohen, R. C., Saykally, R. J. In preparation
66. Fraser, G. T., Lovas, F. J., Suenram, R. D., Matsamura, K. 1990. *J. Mol. Spectrosc.* 144: 97
67. Cohen, R. C., Saykally, R. J. In preparation
68. Smith, L. N., Secrest, D. 1981. *J. Chem. Phys.* 74: 3882
69. von Puttkamer, K., Quack, M., Suhm, M. A. 1988. *Mol. Phys.* 65: 1025; 1987. *Mol. Phys.* 62: 1047
69a. Quack, M., Suhm, M. A. 1990. *Chem. Phys. Lett.* 171: 517
70. Pine, A. S., Howard, B. J. 1986. *J. Chem. Phys.* 84: 590
71. Moazzen-Ahmadi, N., McKellar, A. R. W., Johns, J. W. C. 1988. *Chem. Phys. Lett.* 151: 318; 1989. *J. Mol. Spectrosc.* 138: 282
72. McKellar, A. R. W. 1990. *J. Chem. Phys.* 92: 3261 and references therein
73. Wofford, B. A., Ram, R. S., Quinoncz, A., Bevan, J. W., Olson, W. B., Lafferty, W. 1988. *Chem. Phys. Lett.* 152: 299
74. Lovejoy, C. M., Nelson, D. D. Jr.,

Nesbitt, D. J. 1987. *J. Chem. Phys.* 87: 5621
75. Bunker, P. R., Jensen, P., Karpfen, A., Kofranek, M., Lischka, H. 1987. *J. Chem. Phys.* 92: 7432
76. Karpfen, A., Bunker, P. R., Jensen, P. 1991. *Chem. Phys.* 149: 299
77. Hutson, J. M., Beswick, J. A., Halberstadt, N. 1989. *J. Chem. Phys.* 90: 1337
78. Clary, D. C., Knowles, P. J. 1990. *J. Chem. Phys.* 93: 6334
79. Danby, G. 1989. *J. Phys. B* 22: 1785 and references therein
80. Dykstra, C. E. 1989. *J. Chem. Phys.* 91: 6472
81. Sagarik, K., Ahlrichs, R., Brode, S. 1986. *Mol. Phys.* 57: 1247

Annual Review of Physical Chemistry
Volume 42, 1991

CONTENTS

(*continued*)